

PARTICLE SIZE CHARACTERISTICS OF RIVERBED SEDIMENTS TRANSPORTED BY TIDAL BORE 'BONO' IN KAMPAR ESTUARY, RIAU-INDONESIA

Wisnu Arya Gemilang*, Ulung Jantama Wisna and Guntur Adhi Rahmawan

Research Institute of Coastal Resources and Vulnerability. Ministry of Marine Affairs and Fisheries. Padang, Indonesia.

*Correspondence author: <wisnu.gemilang@yahoo.co.id>

Received: January 2018

Accepted: April 2018

ABSTRACT

The presence of tidal bore in the Kampar River (locally known as 'bono') may influence sedimentation in the Kampar River and its estuary. Understanding sedimentation mechanisms (*e.g.*, erosion, deposition) is important to communities along the Kampar River, which can be studied by analyzing characteristics of grain size distribution. Here, we study riverbed sediment samples collected from 17 stations using an Ekman grab sampler, accompanied by bathymetry and acoustic Doppler current profiler (ADCP) measurements. Grain size data show that the sediments are coarser upstream and gradually finer downstream. Silty sands are predominant in the upstream section of the river, sands in its river body and sandy silts in the downstream. The results indicate the influence of undular bores on grain size characteristics. We also found that the propagation of *bono* and Kampar River's funnel-shaped morphology cause intense scouring events of riverbed sediments. Sortation values that range between 0.33-2.14 suggest unstable currents that result in randomly deposited sediments. The sediment mass transfer per area is positively towards downstream at the low tidal condition. However, after the passage of the bores, the sediment mass transfer area becomes negatively towards upstream.

Keywords: Bono, tidal bore, sediment particle analysis, erosion, sedimentation, Kampar River.

INTRODUCTION

Estuaries represent a unique aquatic environment that is influenced by the physical processes of the seas and land. Tides from the seas trigger the movement of water masses in estuaries in the form of oscillations. These oscillations cause large mixing of waters that stirs organic and inorganic materials, making estuaries a productive fishing ground (Chanson, 2009). Estuaries as a complex aquatic environment are also characterized by dominant sediment deposition from the land (Dyer, 1986).

Sediment deposition plays an important role in the evolution of estuarine and nearshore

morphology. Sediment deposition is governed by tides, waves as well as river dynamics (Dalrymple *et al.*, 1992). The deposition makes imprints on the evolution of estuaries in the forms of channel-bank systems, shoals, mouth bars and nearshore subaqueous deltas. Ultimately, sediments may escape estuaries and are distributed outward along the coast.

A tidal wave that creates tidal bores in some places is a unique natural phenomenon that could enhance sedimentation in upstream rivers by scouring riverbed sediments downstream. The tidal wave propagates upstream due to the difference of hydraulic pressure resulted from changes in tidal elevation. A tidal bore is an

unsteady flow motion triggered by a rapid water level rise at estuaries during the early high tidal condition. High tidal range induces an undular bore when the high tidal elevation moves against the river flow. With time, the leading edge of the tidal wave becomes steeper and steeper, forming a wall of water that is a tidal bore (Docherty and Chanson, 2010).

One of the most well-known tidal bores in Indonesia is the so-called ‘bono’ in Kampar River, Riau. *Bono* is a natural phenomenon generated by the meeting of tidal current and river flow. The funnel shape of the Kampar estuary supports the generation and reinforcement of *bono* (Yulistiyanto, 2009). *Bono* scrapes sands and muds downstream and settles them upstream. Works by Setiady (2010) and Bathara (2013) have analyzed the potential of minerals contained in the bottom sediments of the Kampar River.

This study aims to study sediment characteristics and physical processes controlling sediment dynamics in the Kampar River. Our approach involves analyzing grain size distribution of surface bed-sediments in upstream, river body, and downstream Kampar River.

MATERIALS AND METHODS

Study Site

We conducted surveys in Kampar Estuary (Pelalawan Regency, Riau Province), defined as a river watershed area between 0°40’0”-0°13’20”N and 102°40’0”-103°26’40”E (Figure 1). As many as 17 observation stations were chosen to represent three regions along the river (*i.e.*, upstream, river body, and downstream). In the estuary, there are two Islands existed in the middle of the river namely Muda Island and Serapung Island.

Based on the geological map of Siaksriindrapura and Tanjung Pinang Sumatera, Kampar River lies on top of two rock formations (Cameron *et al.*, 1982). They consist of the younger superficial deposits (Qh) made of clay, silt, gravel, plant waste, peat swamp, coral reefs; and the older superficial deposits (Qp) made of clay, silt, sandy clay, plant waste, and sandy granite.

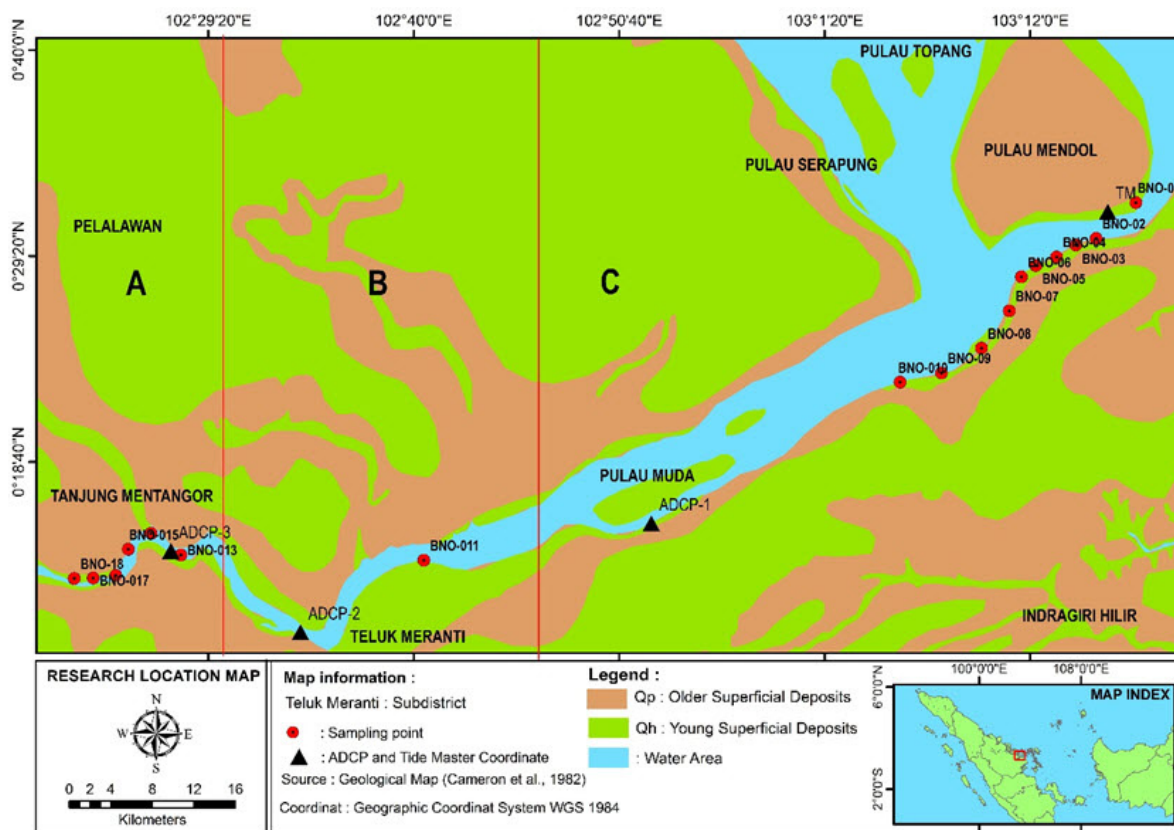


Figure 1. Map of the study site.

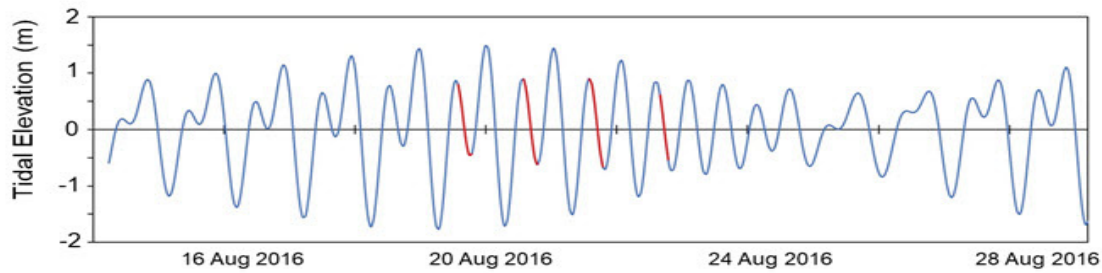


Figure 2. Tidal forecast (in blue) and during riverbed sediment sampling (in red).

Bathymetry Profile

Bathymetry profile closely relates to tidal wave propagation and can also be used to describe sediment dynamics due to tidal oscillations. In the present study, bathymetry data were obtained during field surveys conducted on August 21-23, 2016 by employing an acoustic method (*i.e.*, echotrack CVM Teledyne Odom hydrographic single beam echosounder). The echosounder emitted an acoustic frequency to the bottom of the water to get real-time depth data. The shallow depth of the river and the occurrence of *bono* created challenges in conducting the surveys. For a secondary bathymetry data, we use SRTM30PLUS data retrieved from www.topex.usds.edu on November 29, 2014.

Tide and Current Measurements

Tide and current measurements are essential to describe the generation and characteristics of *bono*, as well as the sediment transport mechanism due to *bono*.

To understand the relationship between the tide and the generation and propagation of

bono upstream, a tide gauge and an ADCP were installed simultaneously. A tide gauge (Valeport tide master) was installed in the estuary of Kampar, specifically in Mendol Island for 33 days (July 23 to August 22, 2016). Tidal forecast during sampling is shown in Figure 2. A Nortek-Aquadopp ADCP was installed in 3 locations at different times between August 20-22, 2016. ADCP was installed at the river bank using a metal pole (Figure 3). Two locations (Muda Island and Teluk Meranti) were chosen to deploy the ADCP based on the local information for observing the arrival of *bono* besides accessibility and work-safety considerations. In Tanjung Mentangor, we used a different ADCP device (RDI Teledyne). The currents were recorded during *bono* in the evening.

The tide gauge data from Mendol Island are analyzed using the admiralty method to yield information on the tidal type, tidal constituents, phase delay and tidal range. The tide data also are used as bathymetry data reduction. One caveat to this is that some inaccuracy may occur because the spring tide in the evening is larger compared to during the sampling time.

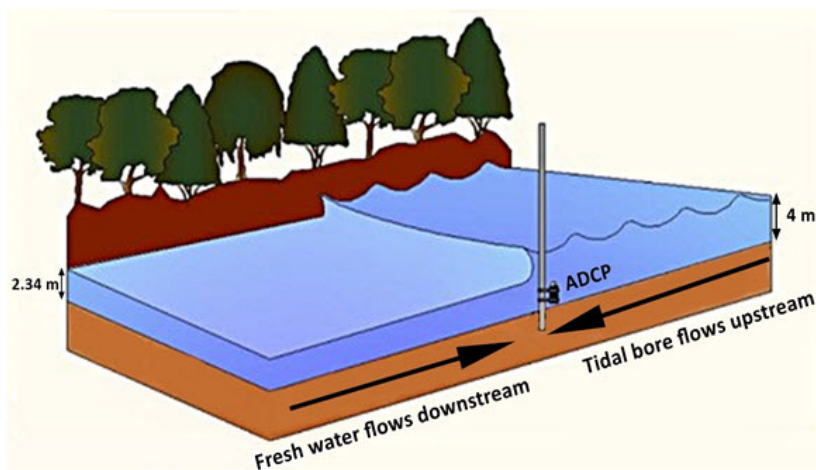


Figure 3. Visualization of ADCP installment in the three points of deployment.

Bathymetry data are corrected by the surface elevation at the time of surveys and from the depth of the transducer. The result of those corrections is the real depth data (Masrukhin *et al.*, 2012) calculated by the following the formula of Nugraha *et al.* (2013):

$$r_t = TWL_t - (MSL + Z_0) \quad (\text{Eq.1})$$

where:

- r_t : The depth reduction at the t time.
- TWL_t : The surface level at the t time
- MSL : Mean sea level
- Z_0 : The ebb water level under MSL

Also, the real depth data are obtained by following the formula below:

$$D = D_t - r_t \quad (\text{Eq.2})$$

where:

- D : The real Depth
- D_t : The depth of the transducer placed
- r_t : The depth reduction at the t time

Riverbed Sediments

Data on riverbed sediments to describe sediment dynamics in the Kampar River were collected on August 20-23, 2016; during a low tidal condition before *bono* propagated upstream. Sediments were sampled approximately 2-5 m from the surface using an Ekman grab sampler (Model 196-B15). Unfortunately, only one

sediment sample could be retrieved from the river body area due to the compact bed sediment and shallow depth that could not be reached by vessel.

We use a statistical approach to determine the mechanisms of sediment transport and deposition by analyzing particle size and sediment type. Particle size separation was conducted using a sieve shaker (pore sizes: >2, 1.4, 1, 0.5, 0.250, 0.090, 0.063 and <0.063 mm). Then, the grain sizes were classified according to Wentworth (1992)'s classification. Sediment type was determined using the ternary diagram classification of Shepard (1954), where grain sizes are categorized into clay (≤ 0.002 mm), silt (0.002-0.0625 mm) and sand (0.0625-2 mm). The statistical parameters used in the sediment analysis are sorting, skewness and kurtosis (Folk and Ward, 1957).

RESULTS

Bathymetry Profile

The funnel shape of the Kampar River gradually alters from upstream to downstream as shown by the river depth and width data (Figures 4 and 5). Bathymetric data analysis shows that the depth of Kampar River ranges from 0.2 to 12.15 m. The shallowest area is in the upstream part, while the deepest area is in the downstream around Mendol Island. In the upstream area around Tanjung Mentangor, the depth only

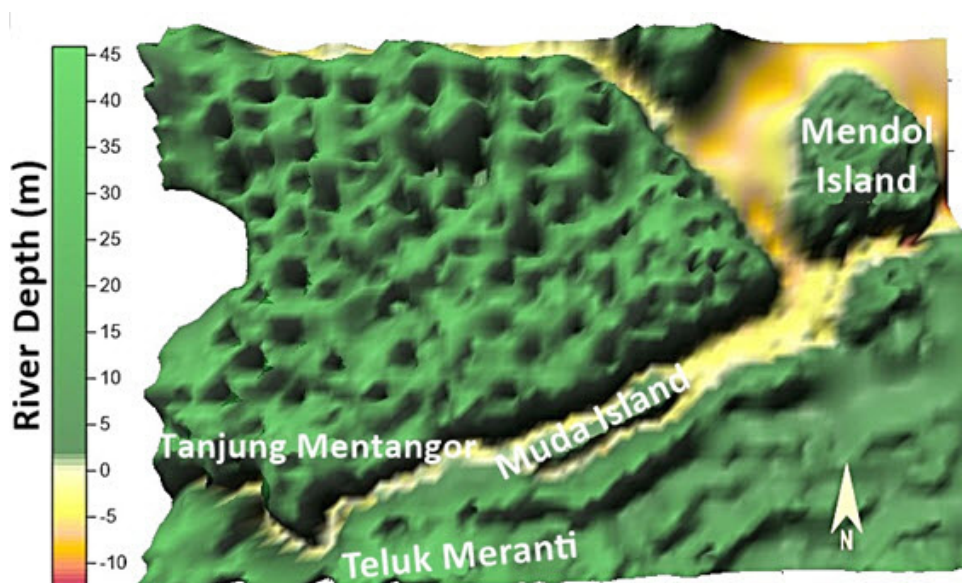


Figure 4. Morphology of Kampar River estuary.

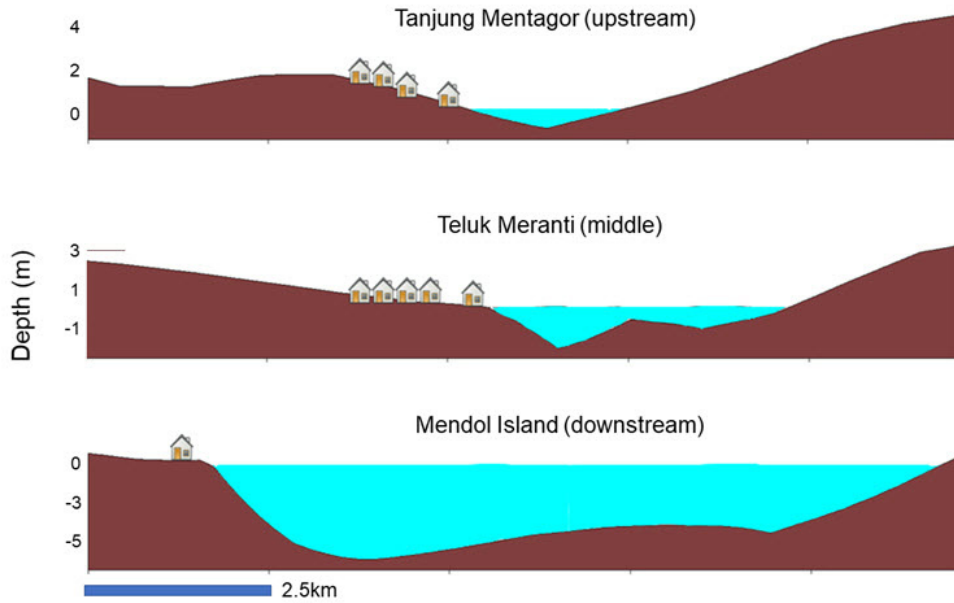


Figure 5. Cross-section of the three observed areas showing the funnel shape of the Kampar River.

reaches 0.2 m and the river width reaches 2.2 km. While in Teluk Meranti, the river depth ranges between 0.3-1.5 m and the river width reaches 4.5 km. In the downstream area, the water depth ranges between 3.2-4.8 m and the river width reaches 10.5 km.

Tide and Current Measurements

Figure 6 shows the current speed and surface elevation data of the three ADCP observation stations (*i.e.*, Muda Island, Teluk Meranti and Tanjung Mentagor).

In Muda Island, surface elevation and current speed enhanced dramatically when *bono* propagated, with the current velocity enhancement

of 0-0.9 m/s. The peak levels differed between *bono* that occurred in the daytime (reached 4 m) versus in the evening (5 m). The currents profile indicates the velocity decreased after *bono* passed Muda Island increased suddenly during maximum ebb before *bono*'s emergence.

Bono's elevation is lower in Teluk Meranti compared to the more downstream Muda Island. The elevation of day-time *bono* reached 1.75 m, while it reached 2.3 m and during *bono* in the evening. In Teluk Meranti, only current data taken in the evening is available (*i.e.*, ebb-current data could not be made) due to its shallow depth. The current speed ranged between 0-0.7 m/s.

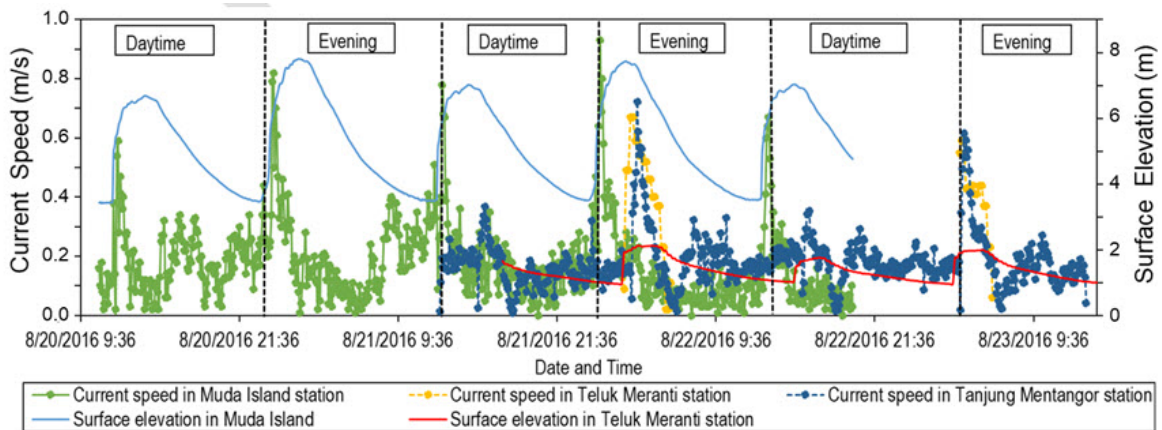


Figure 6. Tidal and currents fluctuation during field measurement.

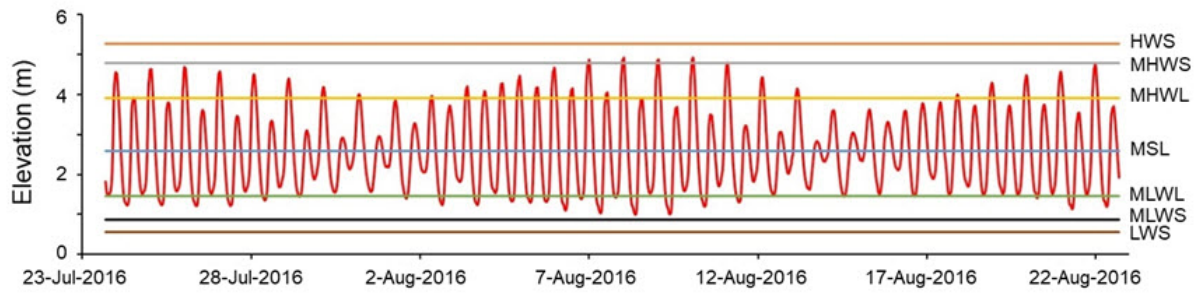


Figure 7. Fluctuation of tidal elevation in the Kampar estuary based on the admiralty analysis.

In Tanjung Mentangor, the current speed during *bono* ranged between 0-0.4 m/s in the daytime and 0-0.7 m/s in the evening. The train of bores decreased dramatically after passing the area. Only current data are available due to the unavailability of the measurement device for the station.

Based on the admiralty analysis, the tidal type of Kampar estuary is a semidiurnal ($F = 0.43$) where flood and ebb tides occur twice a day, but at certain times they could occur once a day (Figure 7). During our surveys, the elevation of the highest water spring (HWS) was 5.27 m and

the lowest water spring (LWS) was 0.56 m. The mean high water spring (MHWS) was 4.79 m, the mean high water level (MHWL) was 3.91 m, the mean low water level (MLWL) was 1.46 m, and the mean low water spring (MLWS) was 0.87 m. These values have not reduced by MSL (2.59 m). These elevations result in tidal fluctuations where the tidal range reached 4.71 m.

Riverbed Sediments

The ternary diagram shows that Kampar River sediments fall under five types of sediment: silt, clayey silt, sandy silt, and silty sand (Figure 8).

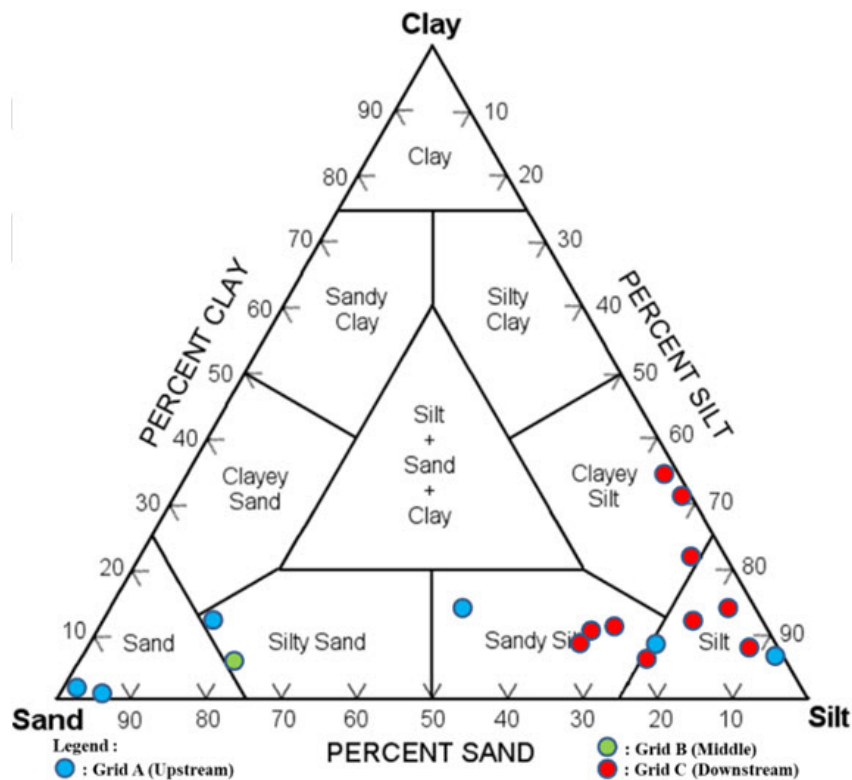


Figure 8. Ternary diagram of 17 riverbed samples taken from the study area.

Table 1. Descriptive statistical analysis for the grain size parameters.

Sample ID	Grid	Grain statistical parameters (ϕ)						
		Sorting	Classification	Skewness	Classification	Kurtosis	Classification	
BNO-01	C	1.43	Poorly sorted	0.37	Strongly fine skewed	4.08	<i>extremely leptokurtic</i>	
BNO-02		1.52	Poorly sorted	-0.62	Strongly coarse	2.52	<i>very leptokurtic</i>	
BNO-03		1.54	Poorly sorted	0.14	Fine skewed	3.76	<i>extremely leptokurtic</i>	
BNO-04		1.61	Poorly sorted	0.25	Fine skewed	2.92	<i>very leptokurtic</i>	
BNO-05		1.56	Poorly sorted	0.29	Fine skewed	2.04	<i>very leptokurtic</i>	
BNO-06		1.99	Poorly sorted	0.29	Fine skewed	1.89	<i>very leptokurtic</i>	
BNO-07		1.43	Poorly sorted	0.18	Fine skewed	2.78	<i>very leptokurtic</i>	
BNO-08		2.14	Very poorly sorted	0.08	near symmetrical	3.02	<i>extremely leptokurtic</i>	
BNO-09		0.88	Moderately sorted	0.04	near symmetrical	1.6	<i>very leptokurtic</i>	
BNO-010		1.54	Poorly sorted	0.25	Fine skewed	3.37	<i>extremely leptokurtic</i>	
BNO-011	B	1.01	Poorly sorted	0.82	Strongly fine skewed	9.02	<i>extremely leptokurtic</i>	
BNO-013		1.08	Poorly sorted	0.22	Fine skewed	5.86	<i>extremely leptokurtic</i>	
BNO-014		0.85	Moderately sorted	0.22	Fine skewed	14.17	<i>extremely leptokurtic</i>	
BNO-015		A	1.99	Poorly sorted	0.07	near symmetrical	3.24	<i>extremely leptokurtic</i>
BNO-016			0.33	Very well sorted	0.27	Fine skewed	31.52	<i>extremely leptokurtic</i>
BNO-017			1.81	Poorly sorted	0.27	Fine skewed	2.01	<i>very leptokurtic</i>
BNO-018			1.61	Poorly sorted	0.23	Fine skewed	2.36	<i>very leptokurtic</i>

Upstream (Grid A) is predominated by silty sand deposition. Bed-sediment in Grid B (a mix-zone between sea and river domination) is predominated by sand. There is a high value of silt sediment in Grid C. Rough materials are also identified in Grid C in the form of sand sediment.

Table 1 shows the description as well as the grouping of sediment texture attribute from a statistical analysis of 17 samples. Sediment texture attribute covers mean (Mz), sorting (SD), skewness (Ski), and kurtosis (KG). Sortation value from all sediment samples started from 0.33 up to 2.14. Generally, it shows the poorly sorted category in all parts of Kampar River morphology. The calculation result of skewness (Ski) shows the fine skewed characteristic ranged

from -0.62 up to 0.82. Kurtosis values ranged from 1.6 up to 14.17. Kurtosis in Grid A (upstream) is categorized into very leptokurtic, while, Grid B and C which represent mix-zone and estuary are categorized into extremely leptokurtic.

Figure 9 shows the comparison between the percentage of the average of grain sizes and current speed during the low tidal condition in our sampling sites.

DISCUSSION

River Morphology and *Bono* Characteristics

The river depth that gradually becomes shallower around Muda and Serapung Island triggers higher *bono* propagation after passing

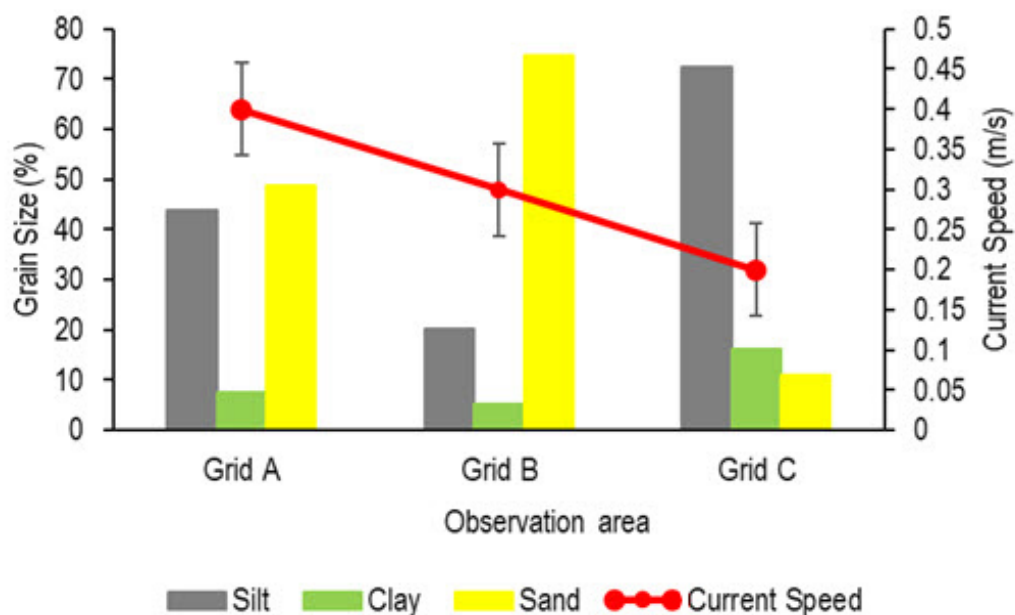


Figure 9. Comparison between the percentage of the average of grain sizes and current speed during the low tidal condition in every grid observation area.

the area. As *bono* arrives, it is separated into two channels with depths of 0.3-1.5 m. Those two separated bores then converge and induce a higher elevation propagating upstream. The drastic elevation change may trigger a more significant water mass transport. In Teluk Meranti, *bono*'s elevation is lower than in Muda Island because of the meander shape of the Kampar river. Also, bottom friction, bed roughness and adverse bed slope, could weaken elevation and speed toward upstream.

The semidiurnal tide in Kampar River propagates in the form of the tidal bore. Previous works reported a semidiurnal angular frequency (M2 and S2) (Rahmawan *et al.*, 2016) with a tidal range up to 5 m where the water level elevation increases as *bono* propagate (Kurniawan *et al.*, 2017). Tidal bores form optimally when the tidal range exceeds 4-6 m and during spring tidal condition. *Bono* emerges twice a day (in the daytime and the evening) in Kampar River with a different wave height due to the mixed semidiurnal tide (Rahmawan *et al.*, 2016). The speed of *bono* depends on surface elevation forming harmonic oscillations along the river.

Bathymetry and tidal dynamics may play a role in sediment resuspension and bed scouring, causing variations between upstream and downstream. During the propagation of *bono*,

scouring mechanisms vary with bathymetry, wave height, speed and sediment type. Erosion at the riverbed provides materials to be carried away by the train of bores, following wave height and propagation speed reductions (Yulistiyanto, 2009). More intense *bono* may trigger more suspended sediments to be carried upstream. Previous work by Wisna *et al.* (2017) suggested that the amounts of suspended sediments after the passage of *bono* in the Kampar River and during a low tidal condition were 98.85 mg/L in downstream, 74.81 mg/L in the river body, and 105.56 mg/L in the upstream. Fine materials would be deposited on the river edge because of wave deformation during the undulation of bores. In turn, bathymetry may influence the peak level of a tidal bore (Prandle, 2006). Bed shear stress, bottom friction, and sediment roughness may inhibit undular bores propagation moving upstream, thus reducing turbulence and scour events.

Grain Size Characteristics

Sortation values shown in this study indicate the poorly sorted category in all parts of Kampar River that may be due to unstable current speed. The finding of ununiform grain sizes in Kampar River is consistent with Bathara (2013).

Fine skewed characteristics of riverbed sediments suggest that the significant input of sediment originates from the river. In this study, sediment sampling was conducted during ebb-tide, therefore explaining the results that lean towards a dominant influence of river flow. Consistently in a gulf setting, Kumar *et al.* (2010) suggest that positive skewness indicates that sediment transport process occurs in the same direction, low energy, and enclosed area.

Very leptokurtic kurtosis indicates that fine grain deposition is dominant that may be due to sortation by a relatively weak transport. This kurtosis category is common for downstream environments (*e.g.*, Irudhayanatan *et al.*, 2011).

Sedimentation Processes

The different sediments between grids A, B, and C in the ternary diagram depict systematic processes of sediment variation from the river to the sea (Figure 10).

Grid A, predominantly silty sand, indicates the influence of river flow carrying the fluvial deposit, erosion, and land debris. This upstream area has non-uniform sediments because of the river domination during ebb tide.

Bed-sediment in Grid B is predominated by sand as the area of mix-zone between sea and river domination. The funnel and meandering shapes of the Kampar river can play a role in enhancing transport energy resulting in coarse sediment transport in the riverbank upstream. The sampling time that was conducted during low tidal condition may influence to some extent. At that time, river flow predominated the sediment transportation, resulting in higher silt domination in the estuary.

The influence of tidal and waves may cause the mixed sediment textures found in each of Grid C sample. The high value of silt sediment in Grid C confirms the higher turbulence in the estuary. Silt sediment sources from upstream. Its domination in the estuary results from water mass transport through the river path during low tidal condition which the flow direction towards downstream. The average of grain sizes has been shown to progressively decrease from the estuary up to river body (silty sand to sandy silt) (Furgerot *et al.*, 2013). In this area, the influence of currents fluctuation is shown by the mixing of fine and coarse grain size (sandy silt). Rough materials are also identified in Grid C in the form of sand sediment. Sand provenance is generally from the sea deposited and sorted by tidal current transport in the estuary.

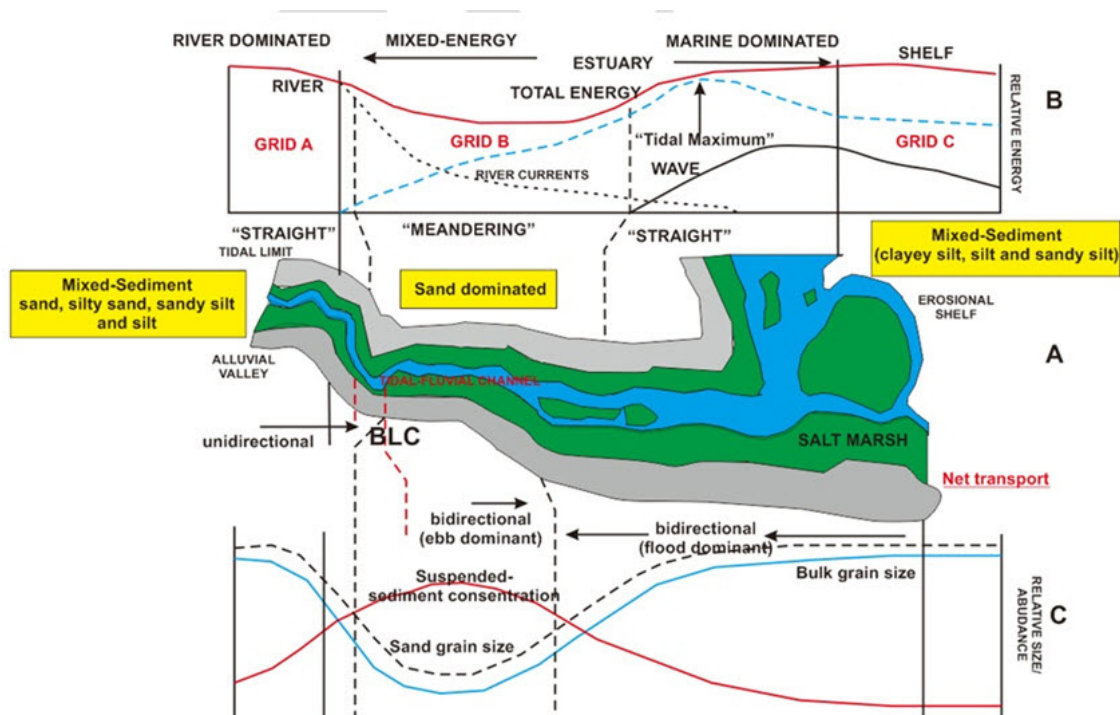


Figure 10. Model of processes in the river-to-marine transition in the Kampar River.

Based on the geological map of Cameron *et al.* (1982), upstream-downstream lithologies are arranged by sediment deposit in the form of silt, clay, as well as the deposition of peat swamp. In this study, we also identified that sediment types in Kampar River are partially amalgamated by plant organic materials.

Hydrodynamic factors influence grain size distribution and statistic parameters. Grain sizes in Grid A to Grid C vary from silty sand to sandy silt. The variation of grain size distribution might be controlled by the current flow (flood and ebb). Grain sizes in Grid A and Grid B are relatively predominated by coarse sediment (sand) upstream indicating the deposited sediment provenance from the sea. The grain size is gradually finer (sandy silt) in Grid C (downstream) due to the deposition of sediment during ebb tide.

Currents fluctuation in Kampar River in the form of river flow and tidal bores causes a random sediment deposition. The hydrodynamic profile causes the unstable sediment deposition. While the coarse sediment is transported upstream by undulation of tidal bores.

CONCLUSION

The morphology of Kampar River (*e.g.*, funnel and meandering shapes as well as bathymetry profile) shapes variations in the riverbed sediments. Grain sizes distribution in the Kampar River shows the graded particle size from upstream to downstream. The current fluctuation produces the unstable deposition along the river shown by the value of sortation (poorly sorted).

Kurtosis in Grid A (upstream) is categorized into very leptokurtic, while Grid B and C (mix-zone and estuary) are categorized into extremely leptokurtic indicating fine sediment domination in those areas. The emergence of *bono* influences the sediment deposition in the upstream and river body characterized by sand domination. Fine sediment identified in the downstream indicating the river-sourced sediment taking over during ebb tide. *Bono* occurrence may influence bed sediment movements along the river which has a significant role in evoking dramatic alteration (in the form of deposition and erosion) in the Kampar River. The weaker the tidal wave propagation, the more sediment deposition upstream.

Further study on net sediment flux, vertical transport as well as vertical resuspension mechanism is needed to better understand the influence of tidal bores on sediment dynamics in the Kampar River.

ACKNOWLEDGMENT

Acknowledgment to Research Institute of Coastal Resources and Vulnerability (LRSDKP) on DIPA 2016 research budget in Kampar, Riau, for Institute of Marine Geology (P3GL) and all those who have assisted in the completion of this research.

REFERENCES

- Bathara, L. (2013). Karakteristik dan potensi sedimen di Muara Sungai Kampar. *Ilmu Perairan (Aquatic Science)*, 7(2), 11-22.
- Cameron, N. R., S. A. Ghazali, and S. J. Thompson. (1982). *Peta Geologi Lembar Saikriindrapura dan Tanjung Pinang, Sumatera*. Pusat Penelitian dan Pengembangan Geologi. Bandung.
- Chanson, H. (2009). Environmental, Ecological and Cultural Impacts of Tidal Bores, Benaks, Bonos, and Burros. IWEH, International Workshop on Environmental Hydraulics, Theoretical, Experimental and Computational solutions, Valencia, 29-30 October 2009. doi: 10.1201/b10999-3.
- Dalrymple, R. W., Zaitlin, B. A., and Boyd, R. (1992). Estuarine facies models: conceptual basis and stratigraphic implications: perspective. *Journal of Sedimentary Research*, 62(6), 1130-1146. doi: 10.1306/d4267f55-2b26-11d7-8648000102c1865d.
- Docherty, N. J., and Chanson, H. (2010). Characterisation of Unsteady Turbulence in Breaking Tidal Bores Including the Effects of Bed Roughness. Hydraulic Model Reports. School of Civil Engineering, The University of Queensland, Report CH76/10. (pp. 100). doi: 10.1061/(asce)ww.1943-5460.0000048.
- Dyer, K. (1986). *Coastal and estuarine sediment dynamics*. John Wiley dan Sons. Chichester. (pp. 342).

- Folk, R. L., and Ward, W. C. (1957). Brazos River bar: a study in the significance of grain size parameters. *Journal of Sedimentary Research*, 27(1), 3-26. doi: 10.1306/74d70646-2b21-11d7-8648000102c1865d.
- Furgerot, L., Mouazé, D., Tessier, B., Perez, L., and Haquin, S. (2013). Suspended sediment concentration in relation to the passage of a tidal bore (See River estuary, Mont Saint Michel Bay, NW France). In: *Proceedings of Coastal Dynamics*. (pp. 671-682). doi: 10.1002/9781119218395.ch4.
- Irudhayanathan, A., Thirunavukkarasu, R., and Senapathi, V. (2011). Grain size characteristics of the Coleroon estuary sediments, Tamilnadu, East coast of India. *Carpathian Journal of Earth and Environmental Sciences*, 6(2), 151-157.
- Kumar, G., Ramanathan, A. L., and Rajkumar, K. (2010). Textural characteristics of the surface sediments of a Tropical mangrove ecosystem Gulf of Kachchh, Gujarat, India. *Indian Journal of Marine Sciences*, 39(3), 415-422.
- Kurniawan, A., Wisha, U. J., Husrin, S., and Karjadi, E. A. (2017). Tidal Bore Generation at the Estuaries of The East Coast of Sumatra. E-proceeding of 37th IAHR World Congress. August 13-18th January 2017, Kuala Lumpur, Malaysia.
- Masrukhin, M. A. A., Sugianto, D. N., and Satriadi, A. (2014). Studi batimetri dan morfologi dasar laut dalam penentuan jalur peletakan pipa bawah laut (Perairan Larangan-Maribaya, Kabupaten Tegal). *Journal of Oceanography*, 3(1), 94-104.
- Nugraha, A. R., Siddhi Saputro, and Purwanto, P. (2013). Pemetaan Batimetri dan Analisis Pasang Surut untuk Menentukan Elevasi Lantai dan Panjang Dermaga 136 di Muara Sungai Mahakam, Sanga-Sanga, Kalimantan Timur. *Semesta Teknika*, 16(1), 21-30.
- Prandle, D. (2006). Dynamical Controls on Estuarine Bathymetry: Assessment Against UK Database. *Estuarine, Coastal and Shelf Science*, 68(1-2), 282-288. Doi: 10.1016/j.ecss.2006.02.009.
- Rahmawan, G. A., Wisha, U. J., Husrin, S., and Ilham. (2016). Analisis batimetri dan pasang surut di muara Sungai Kampar: Pembangkit penalaran gelombang pasang surut undular bore (bono). *J. Geomatics*, 22(2), 57-64. doi: 10.24895/JIG.2016.22-2.573.
- Setiady, D. (2010). Perkiraan potensi cadangan pasir laut yang terdapat di Perairan Muara Kampar Kepulauan Riau. *Buletin Sumber Daya Geologi*. 5(1), 11-16.
- Shepard, F. P. (1954). Nomenclature based on sand-silt-clay ratios. *Journal of Sedimentary Research*, 24(3), 151-158. doi: 10.1306/D4269774-2B26-11D7-8648000102C1865D.
- Wentworth, C. K. (1922). A scale of grade and class terms for clastic sediments. *The Journal of Geology*, 30(5), 377-392.
- Wisha, U. J., Dhiauddin, R., and Kusumah, G. (2017). Remote Estimation of total Suspended Solid (TSS) Transport Affected by Tidal Bore "Bono" of Kampar Big River Estuary Using Landsat 8 OLI Imagery. *Mar. Res. Indonesia*, 42(1), 37-45. doi: 10.14203/mri.v42i1.116.
- Yulistiyanto, B. (2009). Fenomena gelombang pasang Bono di Muara Sungai Kampar. *Jurnal Dinamika Teknik Sipil*, 9(1), 19-26.